JOURNAL OF OPTOELECTRONICS AND ADVANCED MATERIALS, Vol. 11, No. 9, September 2009, p. 1115 - 1121

Grain boundary effects in bulk colossal magnetoresistive (CMR) manganites and manganite/insulator composites: electrical and magnetic properties♣

P. VANDERBEMDEN*, B. VERTRUYEN, M. AUSLOOS, B. RIVAS-MURIAS AND V. LOVCHINOV [a]
University of Liège, SUPRATECS research group, Departments of Electrical engineering & Computer science (B28), Chemistry (B6) and Physics (B5), Sart-Tilman, B-4000 Liège, Belgium.
[a] *Institute of Solid State Physics, Bulgarian Academy of Sciences, 72 Tzarigradsko Chaussee Blvd., 1784 Sofia, Bulgaria.*

In the first part of this paper, we discuss the effects of grain boundaries on the properties of bulk colossal magnetoresistive (CMR) manganites. We compare the electrical resistivity and AC magnetic susceptibility of perovskite La-Ca-Mn-O samples with the same nominal stoichiometry but differing in their microstructure: (i) a single grain sample, (ii) a sample containing two grains and (iii) a polycrystalline sample. Emphasis is placed on information that can be deduced from the measurements in each case. In the second part of the paper, we report the data measured on composite samples containing a CMR phase (La-Ca-Mn-O) and an insulating phase (Mn_3O_4). The results are discussed in the framework of percolation theory. We show how the grain boundaries affect the electrical properties of these materials, and we highlight the crucial role of geometric (demagnetization) effects on the resistance vs. magnetic field measurements.

(Received November 5, 2008; accepted December 15, 2008)

Keywords: Colossal Magnetoresistance, Electrical properties, Magnetic properties, Grain boundaries

1. Introduction

The $Ln_{1-y}A_yMnO_{3-d}$ family (where Ln is a large lanthanide and A generally an alkaline-earth) has been extensively studied since the early nineties [1,2]. These perovskites had already been characterized in the 1950s [3,4], but the interest was renewed by the discovery of colossal magnetoresistance (CMR) properties in some of these materials [5]: the electrical resistance, exhibiting a maximum at a given temperature T_{MI}, is drastically suppressed under the application of a magnetic field. The magnetoresistance is defined as $(R_0-R_H)/R_0$, where R_H and R_0 denote the resistance with and without a magnetic field, respectively. These materials are also characterized by a ferromagnetic-paramagnetic transition at a temperature T_C close to T_{MI}. The magnetic and electrical transport properties of CMR materials are known to be influenced by several parameters, e.g. the Mn^{4+}/Mn^{3+} ratio and lattice distortions [6-9]. In addition to these *intrinsic* parameters, the physical properties are strongly influenced by *extrinsic* parameters, i.e. by the microstructure of the material, as proved by comparative studies of thin films, bulk ceramics, and single crystals [10-12]. On the one hand, the magnetoresistance of single crystals and epitaxial thin films is quite large, but concentrated within a temperature range around the paramagnetic /ferromagnetic transition temperature T_C. On the other hand, polycrystalline materials, either bulk ceramics or thin films, display a significant magnetoresistance at low fields and all temperatures below T_C (Low-Field Magnetoresistance - LFMR). These differences are generally attributed to the presence of grain boundaries in the granular materials, the interfaces between grains being considered as a barrier for the exchange interaction between Mn^{4+} and Mn^{3+} ions. Different models have been proposed to describe the electrical conduction through the grain boundaries (see [13] for a review).

Due to the small size of the grains usually found in bulk polycrystalline materials, it is generally impossible to isolate the behaviour of grain boundaries. Most of the systematic investigations on isolated grain boundaries have thus been carried out on films. Mathur et al., for example, have studied thin film devices that isolate the contribution of a single grain boundary [14]. Such studies on *thin films* allow efficient control of the grain boundary misorientation. The grain boundaries in *bulk* materials, however, may behave differently from those in thin films, in particular because the bulk material is free from crystallographic strains introduced by the film substrate [15].

♣ Paper presented at the International School on Condensed Matter Physics, Varna, Bulgaria, September 2008

In the first part of this paper, we report, summarize and extend our previous work [12,16] on individual grain boundaries in bulk CMR manganites. We compare the electrical resistivity and AC magnetic susceptibility of perovskite La-Ca-Mn-O samples with the same nominal stoichiometry, but differing in their microstructure: (i) a sample containing one single grain, (ii) a sample containing two grains separated by an isolated grain boundary and (iii) a polycrystalline sample.

In the second part of this paper, we report the electrical and magnetic properties of composite samples containing a CMR manganite phase and an insulating oxide secondary phase. The reason for studying such composites is that the presence of the insulating phase forces the electric current to meander through the CMR grains, thereby increasing significantly the contribution of the grain boundaries to the conduction process. This leads, in turn, to an enhancement of the low-field magnetoresistance (LFMR) effect [17-26]. In our group, we are interested in the $La_{0.7}Ca_{0.3}MnO_3$/ Mn_3O_4 composite system, where $La_{0.7}Ca_{0.3}MnO_3$ is the manganite phase and Mn_3O_4 the insulating phase [27,28]. This system is particularly convenient for studying the electrical transport properties of CMR/insulator composites because, as will be shown in the short literature review below, it has unique properties compared to other combinations of materials.

Manganite-insulator composites studied in the literature can be sorted into two groups, depending on the synthesis method: (i) some are sintered at high temperature to achieve *densification*, while (ii) others are submitted to minimal thermal treatment in order to *prevent interdiffusion* between the insulator and manganite phases. A lot of results obtained so far provide evidence of the difficulty of combining both properties (i.e. dense samples with no interdiffusion).

In samples sintered at high temperature, for example, ionic diffusion results in drastic modification of the manganite composition. When the nominal insulating phase is ZrO_2 [17,18] or SiO_2 [19], well-defined phases such as $La_2Zr_2O_7$ or $Ca_2La_8(SiO_4)_6O_2$ are formed at the interfaces between the manganite and ZrO_2 or SiO_2. The La/Ca (or La/Sr) ratio of the manganite phase is modified, as confirmed by a significant decrease of the Curie temperature [17,18]. The alteration of the physical properties of the manganite phase is even more drastic when the insulating phase contains cations that can enter the Mn-O network of the manganite phase [17,18,20] and suppress the double-exchange mechanism responsible for ferromagnetism and metallic-like behaviour of the manganite phase. In brief, thermal treatment at high temperature appears to induce a pronounced composition shift of the manganite composition when the proportion of the insulating phase in the mixture is increased.

Conversely, several authors have prepared composites using a very short thermal treatment in order to prevent these interdiffusion phenomena, e.g. $La_{2/3}Ca_{1/3}MnO_3/Al_2O_3$ (1h 1100°C) [22,23], or other combinations [24-26]. The consequence of the short sintering treatment is a large porosity of the samples and a poor connectivity between the manganite grains.

Taking into account the experimental results mentioned above, we have studied the $La_{0.7}Ca_{0.3}MnO_3$/ Mn_3O_4 composite system, because no compound with Mn/(La+Ca) > 1 exists in the composition, temperature and pressure ranges used during the synthesis of this kind of composite [29]. Therefore, long sintering at high temperature can be used without leading to significant modifications of the manganite phase. Our composite samples were obtained in one step and in a reproducible manner, by spray drying [30] an aqueous solution containing La and Ca in a stoichiometric ratio, and Mn in a suitable excess, followed by high temperature thermal treatment of that precursor. In so doing, composite samples could be prepared with almost constant manganite compositions throughout the series [27]. In this paper, we present the electrical and magnetoresistive properties of such composites, with an emphasis placed on the impact of demagnetization and sample shape effects on the electrical behaviour under a magnetic field.

2. Experimental

The floating zone method was used to prepare a cylindrical rod (length 30 mm, diameter 4mm) of La-Ca-Mn-O CMR material. The details of the synthesis procedure have been described previously [12]. Small samples (typically $0.1 \times 0.2 \times 0.8$ mm³) were excised from the rod using a wire saw. Their microstructures were either single grain (S1), double grain (S2) or polygranular (S3). The cationic composition of the manganite material, determined by EDX analysis, was close to the $La_{0.78}Ca_{0.22}Mn_{0.9}O_x$ stoichiometry, resulting in a slightly lower T_C (~ 190 K) than that which can be expected for the nominal $La_{0.7}Ca_{0.3}MnO_3$ composition (~ 250 K). Note that an oxygen deficiency may also be responsible for a smaller T_C [31].

The composite $La_{0.7}Ca_{0.3}MnO_3/Mn_3O_4$ materials were synthesized from precursor powders obtained by the spray drying technique. This consists of spraying an aqueous solution of metallic cations into droplets, which are dried by a hot air flow. The detailed synthesis process has been described previously (see [27] and references therein).

The samples were characterised by various techniques. Powder X-ray diffraction patterns were collected with a Siemens D5000 diffractometer (Cu K_α radiation). Whole Powder Pattern Decomposition (WPPD) and Rietveld analysis of the X-ray diffraction patterns were performed with Bruker TOPAS software. The morphology of the samples was studied by scanning electron microscopy using a Philips XL30 FEG-ESEM. The cationic composition was checked by an Energy Dispersive X-ray Analysis (EDAX system), coupled to the electron microscope.

The magnetic and electrical properties were measured as a function of temperature and magnetic field using a Quantum Design PPMS (Physical Property Measurement System). Precise AC susceptibility measurements as a

function of temperature were obtained in a home-made AC susceptometer based on a cryocooler [32]. For the analysis of the current transport across one single grain boundary, small electrical contacts were achieved by attaching thin gold wires (33 μm diameter) to the samples using DuPont silver epoxy paste annealed in flowing O_2 for 5 min. The electrical characterization of the most resistive ($\rho > 10^8$ Ωm) composite samples was carried out using a Keithley 617 Programmable Electrometer. Their dielectric properties were measured using a Perkin Elmer 7260 Lock-In amplifier.

3. Results and discussion

In this section, we first present the results obtained on large grain La-Ca-Mn-O CMR materials. Then we turn to analysing the electrical and magnetic characterization of the La-Ca-Mn-O /Mn_3O_4 composites.

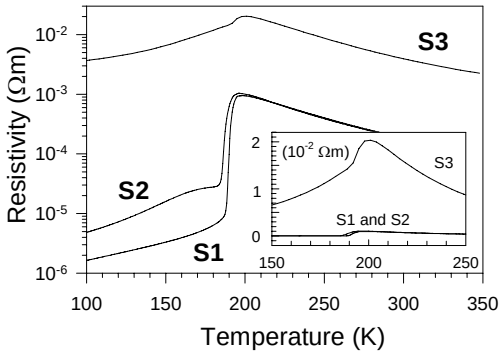

Fig. 1. Temperature dependence of the electrical resistance inside the single grain (S1), across the grain boundary of the double grain (S2) and in the polycrystalline sample (S3). The inset shows the same dataon a linear scale.

3.1. Large grain La-Ca-Mn-O

Fig. 1 shows the temperature dependence of the electrical resistivity measured on 3 samples extracted from the La-Ca-Mn-O rod obtained by the floating zone method. All samples have similar chemical compositions – and display the overall characteristics of a metallic-like - semiconducting-like transition at T_{MI} of the order of 190 K – but differ in their microstructure. As can be seen in Fig. 1, the behaviour of the single grain (S1) markedly differs from that of the double grain (S2) containing one single grain boundary : at $T < T_{MI}$, the resistivity of the single grain (S1) is much lower than that of the boundary, and does not display any inflexion point. Conversely, the double grain sample (S2) exhibits a well-defined shoulder which is the signature of the presence of a single grain boundary in the bulk CMR sample [12]. The resistivity of the poly-granular sample (S3) lies one order of magnitude above that of the S1 and the S2 samples.

In order to characterize the behaviour of a single grain boundary in bulk La-Ca-Mn-O material, we have compared, for the S2 sample, the resistance vs. magnetic field [R(H)] and the magnetization vs. magnetic field [M(H)] curves, both measured at T = 50 K (see Fig. 2). As can be seen, the R(H) data display a significant kink at some magnetic field H* separating the low-field magnetoresistance (LFMR) and the high-field magnetoresistance (HFMR). The H* field corresponds to the saturation field of the S2 sample.

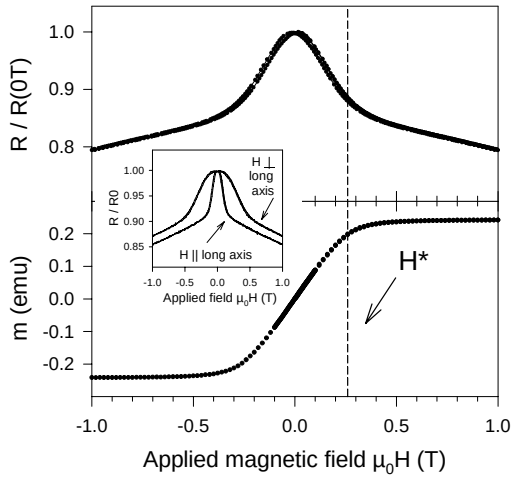

Fig. 2. Magnetic field dependence of (a) the electrical resistance across the grain boundary in the S2 sample and (b) the DC magnetic moment of the S2 sample. The data are measured at 50K. The inset shows, for another double grain sample (S2bis), the influence of the magnetic field orientation on the resistance curves (T=50K).

It is of interest to note that such a behaviour differs from that of a single grain boundary in a thin film [33], for which the kink field H* corresponds to the coercive field of adjacent grains. The mesoscopic model of Evetts et al. [33], assuming that the grain boundary region is polarized by adjacent magnetically soft grains, seems to be appropriate to analyze the behaviour of the single grain boundary in our bulk material [12]. Note also that, if the bulk CMR sample has an anisotropic shape (e.g. parallelipipedic), the saturation field for H perpendicular to the sample long axis is larger than for H parallel to the long axis, because of demagnetizing effects. As a result, the kink field H* (coinciding with the saturation field), is dependent on the field direction with respect to the sample's long axis. This is illustrated in the inset of Fig. 2.
Now we examine the AC magnetic behaviour of the three samples. Fig. 3 shows the temperature dependence of the in-phase AC susceptibility measured at 1 mT and 1 kHz, without a bias DC magnetic field. The data measured on 3 samples display the characteristics of a classical ferromagnetic – paramagnetic phase transition [34] at T_C ~ 190 K. We emphasize that the differences in the AC susceptibility signal at $T < T_C$ are related to the sample dimensions (i.e. their demagnetization factor D) and *not* to

their microstructure [16]. This is visible for the S2 sample which was re-measured under the same experimental conditions but with a magnetic field oriented at 90° (dashed S2' curve in Fig. 3) with respect to the original measurement (plain S2 curve). In the ferromagnetic phase, the measured (apparent) susceptibility is bounded to a maximum value roughly equal to 1/D. The resulting signal is almost temperature-independent, as observed indeed in Fig. 3 for $T < T_C$. Assuming that $\chi' \sim 1/D$, one can extract the demagnetization factors for each sample, and the results are in agreement with the D values estimated from the sample dimensions [16].

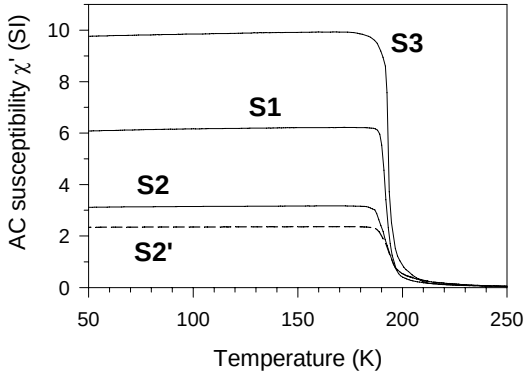

Fig. 3. In-phase AC susceptibility measured at 1 mT and 1 kHz for the S1, S2 and S3 samples. The dotted line (S2') shows, for the S2 sample, the data measured with the magnetic field perpendicular to the sample long axis.

In order to obtain an AC magnetic signal which is not bounded by geometric effects, a DC magnetic field can be applied in addition to the AC field. In such a case (Fig. 4), the main AC susceptibility signal is drastically suppressed, allowing the emergence of a universal signal contribution arising from critical fluctuations [34,35]. For the single grain (S1) and the polygranular (S3) samples (not shown here), a well-defined peak appears at around the transition temperature, as usually observed in dilute magnetic systems and CMR ceramics [34-37].

Remarkably, the double grain sample (S2) displays a shoulder structure (see the arrows in the inset of Fig. 4) which is not observable in the S1 and the S3 samples. This peculiar behaviour can be attributed to a slight difference (~3K) in the critical temperatures of the two grains of the S2 sample [16].

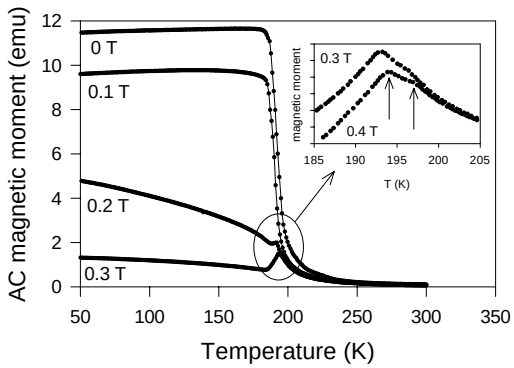

Fig. 4. AC in-phase magnetic moment of the double grain sample (1 mT and 1 kHz) under various superimposed DC fields ranging from 0 to 0.4 T. The inset shows the shoulder structure.

In the polygranular (S3) sample containing numerous small grains, one can also expect small T_C inhomogeneities, but the magnetic signal is averaged over a length scale which is much larger than the grain size. The result shown in Fig. 4 is particularly significant, and demonstrates that specific features can be observed in the magnetic properties when the size of the grains is comparable to that of the sample.

3.2. Composite materials

A series of dense composite $La_{0.7}Ca_{0.3}MnO_3$/ Mn_3O_4 samples with different proportions of the two phases was synthesised using a one-step spray-drying synthesis followed by a long thermal treatment at 1300°C. The chemical composition of the manganite (LCMO) phase was shown [27] to be weakly influenced by the proportion of the insulating phase (Mn_3O_4). The typical microstructures of two composite samples are shown in Fig. 5 : for a small Mn_3O_4 content, the material displays Mn_3O_4 islands in a LCMO matrix (Fig. 5a), whereas for a higher Mn_3O_4 content, the microstructure consists of a labyrinthine pattern of the two phases (Fig. 5b). As shown in Fig. 5, the materials inevitably exhibit some porosity. Density measurements by the Archimedes method allowed us to determine the volume fraction of each phase, i.e. the LCMO phase, the Mn_3O_4 phase and the pores. The results hereafter are discussed in terms of the dimensionless manganite (LCMO) volume fraction, denoted by f_M ($0 < f_M < 1$).

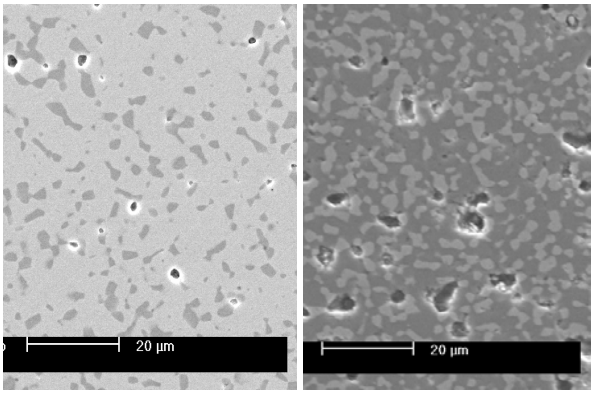

Fig. 5. Electron micrographs of polished cross-sections of composite samples with two LCMO volume fractions. (a) : f_M ~ 0.83; (b) : f_M ~ 0.34. The light and dark grey regions correspond to LCMO and Mn_3O_4 respectively.

Fig. 6 shows the resistivity vs. temperature curves for the composites containing various LCMO volume fractions f_M = 0.92, 0.57, 0.43, 0.26, 0.21 and 0.19. Note that a logarithmic scale is used for the resistivity axis. The 5 composite materials with the largest LCMO volume fractions exhibit a clear transition from a semiconducting-like behaviour above T_{MI} (~ 250 K) to a metallic-like behaviour below T_{MI}. On decreasing the LCMO content from 0.92 to 0.21, the bump appearing at low temperature (100K < T < 200K) progressively grows, clearly indicating an increasing contribution of the grain boundary contribution in the polycrystalline manganite [12,33]. The composite containing ~ 19% LCMO does not display any resistive transition in the temperature range where the resistivity could be measured accurately in our experimental system ($\rho < 10^9$ Ω.cm). The sharp increase in resistivity (4 orders of magnitude) indicates the existence of a percolation threshold. This feature is visible in the inset of Fig. 6, showing the resistivity measured at T = 300 K as a function of the manganite volume fraction f_M. The percolation threshold is found to be ~ 0.18 ± 0.01. This value is remarkably close to the values calculated for regular three-dimensional periodic lattices for which the critical volume fractions lie in the range 0.16 ± 0.02 [38]. This suggests that the spray drying process used for synthesizing our composites produces a random "auto-organization" of the two phases in the samples [27].

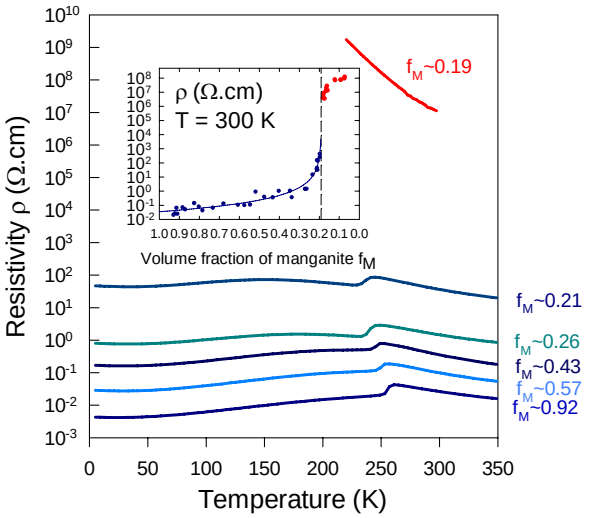

Fig. 6. Temperature dependence of the electrical resistivity of composite samples containing LCMO volume fractions ranging between 0.92 and 0.19. Inset : resistivity at 300K as a function of the LCMO volume fraction.

As can be seen in Fig. 7, the presence of a small proportion of a conducting LCMO phase (f_M ~ 0.09) in the Mn_3O_4 composite also has a profound impact on the room-temperature dielectric properties. The presence of the manganite phase produces an extrinsic interfacial or space-charge polarization mechanism, resulting in an increase in the real part of the permittivity [39,40].

The enhancement of the LFMR effect for low manganite volume fractions is observable in Table 1, which compares the magnetoresistance measured at an applied field of 0.2 T for 3 composite samples with different proportions of the two phases. The material with f_M ~ 0.26 is seen to exhibit a relatively large magnetoresistance of ~ 17 %, attributable to the contribution of grain boundaries to the conduction process.

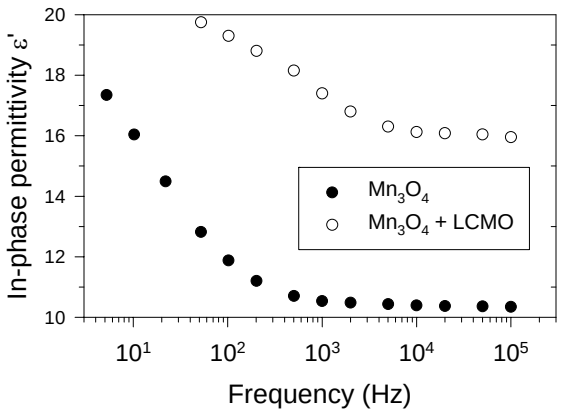

Fig. 7. Frequency dependence of the in-phase permittivity for pure Mn_3O_4 and for a composite sample

with a LCMO volume fraction ~ 0.09.

Table 1. Magnetoresistance at T = 10 K and $\mu_0 H$ = 0.2 T for 3 composite samples.

Manganite volume fraction (f_M)	MR (%) T = 10K - $\mu_0 H$ = 0.2 T
0.92	6.0 %
0.60	7.8 %
0.26	17.2 %

Fig. 8 shows a typical resistance vs. magnetic field plot, measured on a composite material (f_M ~ 0.26) at T = 10 K, when the magnetic field is cycled with an amplitude of 0.2 T. The graph shows an enlargement between -0.1 T and 0.1 T and the arrows indicate the scan directions. A significant hysteresis effect is observable. Unlike the "classical" hysteresis usually reported in single phase polycrystalline manganite samples [30,41], the behaviour depicted in Fig. 8 is unusual : when the applied magnetic field is scanned from positive to negative values, the resistance peak occurs at a *positive* magnetic field. This effect can be attributed to the fact that Mn_3O_4 is a hard ferrimagnet for T < 42 K [42], whereas the LCMO phase is a soft ferromagnet in this temperature range. The hysteretic behaviour could be explained [28] by assuming that, at the resistivity maximum, the magnetization of the composite is due to that of Mn_3O_4 only. The maximum occurs when the internal magnetic field is zero, i.e. when the demagnetizing field of the Mn_3O_4 phase cancels the applied field in the LCMO phase. The fact that the demagnetization field, strongly dependent on the sample shape, is responsible for this unusual behaviour emphasizes the considerable influence of geometric effects on the magnetoresisitive properties of ferromagnetic/ferrimagnetic composites.

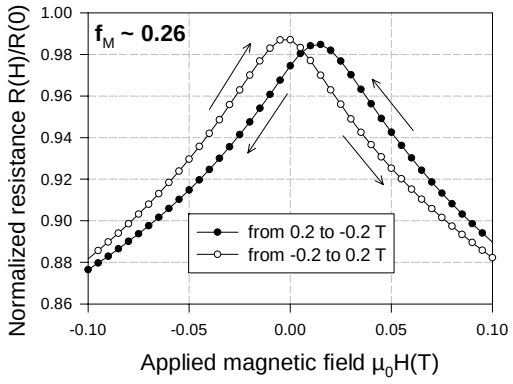

Fig. 8. Magnetic field dependence of the resistivity of a composite sample having f_M ~ 0.26. The temperature is 10 K and the applied field is cycled between 0.2 and – 0.2 T.

4. Conclusions

The set of results presented above highlights the effects of grain boundaries on the electrical and magnetic properties of bulk CMR manganites and manganite / insulator composites. In addition to the influence of the microstructure, geometric effects have been shown to sometimes play a significant role. It is therefore recommended that the properties of samples of different shapes should always be investigated, in order to determine whether the demagnetization effects are relevant. Finally, we emphasize the importance of explicitly reporting the field scan directions in hysteresis curves.

Acknowledgements

Part of this work was supported by the European Network of Excellence FAME. The authors would like to thank A. Delvaux for preparing some of the samples and J.-F. Fagnard for carrying out careful electrical measurements. Electron microscopy was performed in the Catμ microscopy centre (ULg, Belgium). We thank ULg and FRS-FNRS (Belgium) for cryofluid and equipment grants. This work is part of a collaboration programme financed by the Commissariat Général aux Relations Internationales, Belgium and the Bulgarian Academy of Sciences.

References

[1] P. K. Siwach, H. K. Singh, O. Srivastava, J. Phys.: Condens. Matter **20**, 273201 (2008).
[2] J. M. D. Coey, M. Viret, S. von Molnar, Adv. Phys. **48**, 167 (1999).
[3] E. O. Wollan, W. C. Koehler, Phys. Rev. **100**, 545 (1955).
[4] G. H. Jonker, J. H. Van Santen, Physica **XVI**, 337 (1950).
[5] S. Jin, T. H. Tiefel, M. McCormack, R. A. Fastnacht, R. Ramesh, L. H. Chen, Science **264**, 413 (1994).
[6] B. Raveau, A. Maignan, C. Martin, M. Hervieu, Chem. Mater. **10**, 2641 (1999).
[7] Y. Tokura, Y. Tomioka, J. Magn. Magn. Mater. **200**, 1 (1999).
[8] B. Vertruyen, A. Rulmont, R. Cloots, M. Ausloos, J.-F. Fagnard, S. Dorbolo, Ph. Vanderbemden, J. Magn. Magn. Mater. **268**, 364 (2004).
[9] B. Vertruyen, D. Flahaut, S. Hébert, A. Maignan, C. Martin, M. Hervieu, B. Raveau, J. Magn. Magn. Mater. **280**, 75 (2004).
[10] C. S. Hong, W. S. Kim, E. O. Chi, K. W. Lee, N. H. Hur, Chem. Mater. **12**, 3509 (2000).
[11] G. J. Snyder, R. Hiskes, S. DiCarolis, M. R. Beasley, T. H. Geballe, Phys. Rev. B **53**, 14434 (1996).
[12] B. Vertruyen, R. Cloots, A. Rulmont, G. Dhalenne, M. Ausloos, Ph. Vanderbemden, J. Appl. Phys. **90**, 5692 (2001)

[13] M. Ziese, Rep. Prog. Phys. **65**, 143 (2002).
[14] N. D. Mathur, G. Burnell, S. P. Isaac, T. J. Jackson, B.-S. Teo, J. L. MacManus-Driscoll, L. F. Cohen, J. E. Evetts, M. G. Blamire, Nature **387**, 266 (1997).
[15] Y. A. Soh, G. Aeppli, N. D. Mathur, M. G. Blamire, Phys. Rev. B **63**, 020402(R) (2001).
[16] Ph. Vanderbemden, B. Vertruyen, A. Rulmont, R. Cloots, G. Dhalenne, M.Ausloos, Phys. Rev. B **68**, 224418 (2003).
[17] D. Das, A. Saha, S. E. Russek, R. Raj, D. Bahadur, J. Appl. Phys. **93**, 8301 (2003).
[18] Z. C. Xia, S. L.Yuan, W. Feng, L. J. Zhang, G. H. Zhang, J. Tang, L. Liu, D. W. Liu, Q. H. Zheng, L. Chen, Z. H. Fang, S. Liu, C. Q. Tang, Solid State Commun. **127**, 567 (2003).
[19] D. Das, P. Chowdhury, R. N. Das, C. M. Srivastava, A. K. Nigam, D. J. Bahadur, J. Magn. Magn. Mater. **238**, 178 (2002).
[20] D. Das, C. M. Srivastava, D. Bahadur, A. K. Nigam, S. K. Malik, J. Phys.: Condens. Matter **16**, 4089 (2004).
[21] P. Kameli, H. Salamati, M. Eshraghi, M. R. Mohammadizadeh, J. Appl. Phys. **98**, 043908 (2005).
[22] L. E. Hueso, J. Rivas, F. Rivadulla, M. A. Lopez-Quintela, J. Non-Cryst. Solids **287**, 324 (2001).
[23] L. E. Hueso, J. Rivas, F. Rivadulla, M. A. Lopez-Quintela, J. Appl. Phys. **89**, 1746 (2001).
[24] D. K. Petrov, L. Krusin-Elbaum, J. Z. Sun, C. Feild, P. R. Duncombe, Appl. Phys. Lett. **75**, 995 (1999).
[25] A. Gupta, R. Ranijt, C. Mitra, P. Raychaudhuri, R. Pinto, Appl. Phys. Lett. **78**, 362 (2001).
[26] L. Balcells, A. E. Carrillo, B. Martinez, J. Fontcuberta, Appl. Phys. Lett. **74**, 4014 (1999).
[27] B. Vertruyen, R. Cloots, M. Ausloos, J.-F. Fagnard, Ph. Vanderbemden, Phys. Rev. B **75**, 165112 (2007).
[28] B. Vertruyen, R. Cloots, M. Ausloos, J.-F. Fagnard, Ph. Vanderbemden, Appl. Phys. Lett. **91**, 062514 (2007).
[29] JCPDS, Powder Diffraction File Database.
[30] B. Vertruyen, A. Rulmont, R. Cloots, J.-F. Fagnard, M. Ausloos, I. Vandriessche, S. Hoste, J. Mater. Sci. **40**, 117 (2005).
[31] K. Dörr, J. M. De Teresa, K.-H. Müller, D. Eckert, T. Walter, E. Vlakhov, K. Nenkov, L. Schultz, J. Phys.: Condens. Matter **12**, 7099 (2000).
[32] Ph. Vanderbemden, Cryogenics **38**, 839 (1998).
[33] J. E. Evetts, M. G. Blamire, N. D. Mathur, S. P. Isaac, B.-S. Teo, L. F. Cohen, J. L. MacManus-Driscoll, Philos. Trans. R. Soc. London, Ser. A **356**, 1593 (1998).
[34] J. H. Zhao, X. Z. Zhou, A. Peles, S. H. Ge, H. P. Kunkel, G. Williams, Phys. Rev. B **59**, 8391 (1999).
[35] G. Williams, in Magnetic Susceptibility of Superconductors and Other Spin Systems, edited by R.A. Hein et al. (Plenum, New York, 1991), p. 503.
[36] A. Peles, H. P. Kunkel, X. Z. Zhou, G. Williams, J. Phys.: Condens. Matter **11**, 8111 (1999).
[37] J. H. Zhao, H. P. Kunkel, X. Z. Zhou, G. Williams, J. Phys.: Condens. Matter **13**, 5785 (2001).
[38] H. Scher, R. Zallen, J. Chem. Phys. **20**, 325 (1970).
[39] A. von Hippel, Dielectrics and Waves (Artech House, London, 1954).
[40] J. Rivas, J. Mira, B. Rivas-Murias, A. Fondado, J. Dec, W. Kleeman, M. A. Señaris-Rodríguez, Appl. Phys. Lett. **88**, 242906 (2006).
[41] X. W. Li, A. Gupta, G. Xiao, G. Q. Gong, Appl. Phys. Lett. **71**, 1124 (1997).
[42] K. Dwight, N. Menyuk, Phys. Rev. **119**, 1470 (1960).

*Corresponding author: Philippe.Vanderbemden@ulg.ac.be